



SAFETY ANALYSIS AGAINST TSUNAMI ATTACKS AT ULCHIN NUCLEAR POWER PLANT SITE

Sobeom Jin¹, Seung Gyu Hyun², Taek-Gue Kwon³, Jeong-Wook Seo⁴, Y.-S. Cho⁵

¹ Principal Researcher, Korea Institute of Nuclear Safety, 62 Gwahak-ro, Yuseong-gu, Daejeon 305-338, Korea (jinsb@kins.re.kr)

² Senior Researcher, Korea Institute of Nuclear Safety, 62 Gwahak-ro, Yuseong-gu, Daejeon 305-338, Korea (mgodo@kins.re.kr)

³ General Manager, Korea Hydro and Nuclear Power Co., LTD, 255 Yangjung-ro, Gyeongju-si, Gyeongsangbukdo 780-935, Korea (bimil@khnp.co.kr)

⁴ Graduate Student, Dept. of Civil and Environmental Engineering, Hanyang University, 222 Wangsimni-ro, Seongdong-gu, Seoul 133-791, Korea (jjap1212@hanyang.ac.kr)

⁵ Corresponding Author, Professor, Dept. of Civil and Environmental Engineering, Hanyang University, 222 Wangsimni-ro, Seongdong-gu, Seoul 133-791, Korea (ysc59@hanyang.ac.kr)

ABSTRACT

A coupled numerical model based on the shallow-water theory is employed to analyze the safety of the Ulchin Nuclear Power Plant site against three historical and eleven virtual tsunami attacks. The numerical model consists of a transoceanic propagation and an inundation models both solved by finite difference methods. By using a dispersion-corrected scheme, the numerical dispersion is manipulated to replace the physical dispersion of the linear Boussinesq equations in the propagation model. In the inundation model, the nonlinear shallow-water equations including bottom friction are employed to describe the run-up and run-down process of tsunamis near the shoreline. The safety of the Ulchin Nuclear Power Plant site is estimated by predicting the maximum tsunami heights.

INTRODUCTION

Recently, several catastrophic tsunamis have been occurred around the Pacific Ocean rim. Among them, the East Japan Tsunami (2011 Tohoku Tsunami, IOC/UNESCO; Tohoku Pacific Earthquake Tsunami, Japan side) occurred on March 11, 2011 has attracted world-wide attention due to the accident at the Fukushima Dai-ichi Nuclear Power Plant site. The accident is still going on progress.

A number of tsunami-triggering earthquakes occur in subduction zones around the Pacific Ocean area including the East Sea surrounded by Korea, Japan and Russia. Furthermore, according to the Korea Meteorological Administration (<http://www.kma.go.kr>), the number of submarine earthquakes around the Korean Peninsula has increased recently as 30 times in 2009, 18 times in 2010, 37 times in 2011. In the East Sea, there were three major tsunami events occurred in 1964, 1983 and 1993. Among them, the Central East Sea Tsunami occurred in 1983, in special, caused huge losses of human lives and property damage at Korean and Japanese coastal communities.

There are several nuclear power plants now under operation and more plants will be built along the Eastern Coast of the Korean Peninsula. These nuclear power plant sites may be vulnerable to unexpected tsunami attacks. Thus, in order to prevent unusual devastating damage from tsunamis, it is essential to be constructed in a safety zone along the coastline. This safety zone can be designated by the maximum run-up heights of tsunami, which may play a significant role when determining the elevation of a nuclear power plant site.

In this study, the safety of the Ulchin Nuclear Power Plant site against tsunami attacks is investigated by predicting the maximum run-up heights. Three historical and eleven virtual tsunami events are employed to simulate propagation of tsunami across the East Sea. The numerical model for

tsunamis simulation, which composed of a model for simulating the propagation of tsunami across the East Sea and the other model for simulating run-up process of tsunami, is based on the shallow-water theory.

NUMERICAL MODEL FOR TSUNAMI SIMULATION

When tsunamis propagate over a long distance, the dispersion effects may play an important role in tsunami propagation and should be considered in modeling. Thus, in the numerical simulation of tsunami propagation, governing equations that address the dispersion effects, the linear Boussinesq equations are adequate (Imamura et al., 1988). However, the frequency dispersion terms of the linear Boussinesq equations have difficulty in discretizing due to the high-order derivatives. In this study, the linear shallow-water equations are used instead of the linear Boussinesq equations as the governing equations. Also, a dispersion-corrected scheme that can account for the dispersion effects is applied to the linear shallow-water equations (Cho, 1995; Cho et al., 2007). The difference equations can be written in the following form.

$$\frac{\zeta_{i+1/2,j}^{n+1/2} - \zeta_{i,j}^{n-1/2}}{\Delta t} + \frac{P_{i+1/2,j}^n - P_{i-1/2,j}^n}{\Delta x} + \frac{Q_{i,j+1/2}^n - Q_{i,j-1/2}^n}{\Delta y} = 0 \quad (1)$$

$$\begin{aligned} & \frac{P_{i+1/2,j}^{n+1} - P_{i+1/2,j}^n}{\Delta t} + gh_{i+1/2,j} \frac{\zeta_{i+1,j}^{n+1/2} - \zeta_{i,j}^{n+1/2}}{\Delta x} \\ & + \frac{\alpha}{12\Delta x} gh_{i+1/2,j} \left[\zeta_{i+2,j}^{n+1/2} - 3\zeta_{i+1,j}^{n+1/2} + 3\zeta_{i,j}^{n+1/2} - \zeta_{i-1,j}^{n+1/2} \right] \\ & + \frac{\gamma}{12\Delta x} gh_{i+1/2,j} \left[\left(\zeta_{i+1,j+1}^{n+1/2} - 2\zeta_{i+1,j}^{n+1/2} + \zeta_{i+1,j-1}^{n+1/2} \right) - \left(\zeta_{i,j+1}^{n+1/2} - 2\zeta_{i,j}^{n+1/2} + \zeta_{i,j-1}^{n+1/2} \right) \right] = 0 \end{aligned} \quad (2)$$

$$\begin{aligned} & \frac{Q_{i,j+1/2}^{n+1} - Q_{i,j+1/2}^n}{\Delta t} + gh_{i,j+1/2} \frac{\zeta_{i,j+1}^{n+1/2} - \zeta_{i,j}^{n+1/2}}{\Delta x} \\ & + \frac{\alpha}{12\Delta y} gh_{i,j+1/2} \left[\zeta_{i,j+2}^{n+1/2} - 3\zeta_{i,j+1}^{n+1/2} + 3\zeta_{i,j}^{n+1/2} - \zeta_{i,j-1}^{n+1/2} \right] \\ & + \frac{\gamma}{12\Delta y} gh_{i,j+1/2} \left[\left(\zeta_{i+1,j+1}^{n+1/2} - 2\zeta_{i,j+1}^{n+1/2} + \zeta_{i-1,j+1}^{n+1/2} \right) - \left(\zeta_{i+1,j}^{n+1/2} - 2\zeta_{i,j}^{n+1/2} + \zeta_{i-1,j}^{n+1/2} \right) \right] = 0 \end{aligned} \quad (3)$$

where ζ is the free surface displacement, P and Q are the depth-averaged volume fluxes in the x - and y -axis directions, respectively, g is the gravity acceleration and h is the still-water depth. The spatial grid sizes in the x - and y -axis directions are represented by Δx and Δy , respectively, and the time step size is symbolized by Δt .

Because a staggered grid system is used, the free surface displacement is calculated in the center grid, and volume fluxes P and Q are calculated in the boundary grid. The dispersion-corrected coefficients, α and γ are determined by a relation of depth, spatial grid size and time step size. The following equation is the relation of α and γ .

$$\alpha = \frac{4h^2 + gh(\Delta t)^2 - (\Delta x)^2}{(\Delta x)^2}, \quad \gamma = \alpha + 1 \quad (4)$$

The proposed scheme uses the numerical dispersion generated from the finite difference approximation to mimic the frequency dispersion term of the linear Boussinesq equations. Thus, even if the linear shallow-water equations are used to govern tsunami propagation, the application of the dispersion-corrected scheme results in numerical dispersion effects comparable to the physical dispersion effects of the linear Boussinesq equations (Cho et al., 2007).

As a tsunami approaches the coastal area, the wave length of the incident tsunami becomes shorter and the amplitude becomes larger. Thus, the nonlinear convective inertia force and bottom friction become increasingly important, while the significance of the frequency dispersion diminishes. The nonlinear shallow-water equations including the bottom frictional effects are adequate for describing the flow motion in the coastal zone (Kajiura and Shuto, 1990). The governing equations and corresponding finite difference schemes are not repeated here and detailed description of the inundation model can be found in Cho (1995).

INITIAL CONDITION FOR THE TSUNAMI SIMULATION

In this study, initial conditions for the tsunami simulation are three historical tsunami and eleven virtual tsunami events. These three historical tsunami events occurred in 1964, 1983 and 1993. The Korean Peninsula Energy Development Organization (1999) identified 11 points that have a high probability of earthquake occurrence. The location of initial conditions for the tsunami simulation is represented in Figure 1. The location and the applied earthquake fault parameters of three historical tsunamis and eleven virtual tsunamis are given in Table 1. In table 1, H is the depth of the fault plane, θ is the strike angle, δ is the dip angle, γ is the slip angle, L is the length of fault, W is the width of fault, D is the dislocation of fault, and M is the magnitude of the earthquake. The depth of the fault plane, the dip angle, and the slip angle were obtained by using the model of Mansinha and Smylie (1971).

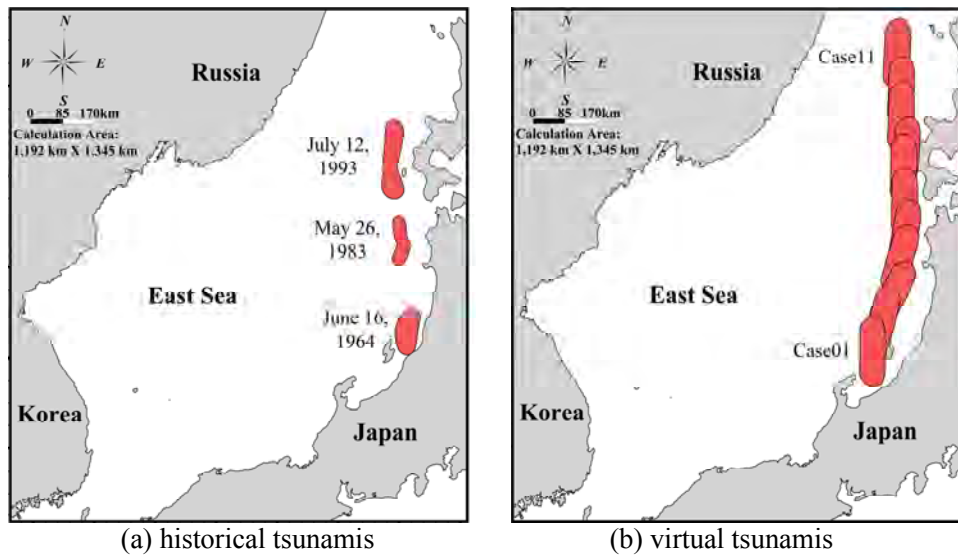


Figure 1. Locations of earthquake epicenters for historical and virtual tsunamis

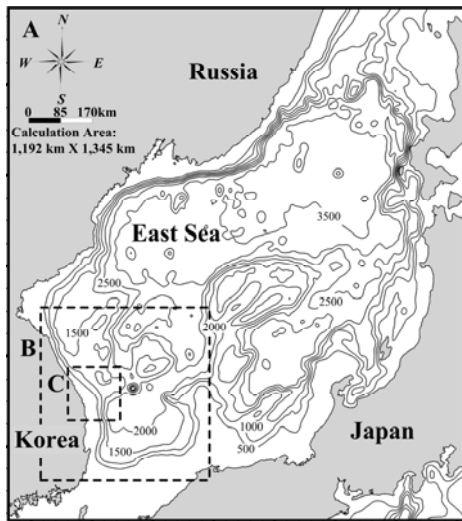
NUMERICAL SIMULATION

To obtain accurate results, it is essential to use a fine grid mesh size that is smaller than 5 to 10m in simulation of run-up process. Thus, the dynamic linking method should be used to obtain accuracy and computational efficiency in a large region such as the East Sea. In the dynamic linking method, coarser grids in deep sea are dynamically linked with the grid having 1/3 size in shallower region. In computation,

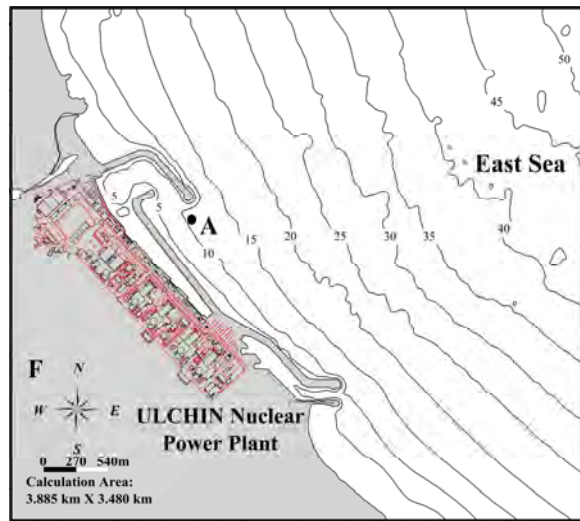
the water level and discharge are exchanged with each other to satisfy the dynamic equilibrium. The process that composes and links each region having different grid sizes is iterated until the target area is described with a proper resolution. The computational domains divided into six regions in this study, the bathymetry of region A and F are represented in Figure 2.

Table 1: Location and fault parameters for historical and virtual tsunamis

Date	Location		H (km)	θ (°)	δ (°)	γ (°)	L (km)	W (km)	D (m)	M
	Long. (°E)	Lat. (°N)								
1964	139.42	38.74	1	189	56	90	80	30	3.30	7.5
1983	138.84	40.21	2	22	40	90	40	30	7.60	7.7
	139.02	40.54	3	355	25	80	60	30	3.05	
1993	139.30	42.10	5	163	60	105	24.5	25	12.00	7.8
	139.25	42.34	5	175	60	105	30	25	2.50	
	139.40	43.13	10	188	35	80	90	25	5.71	
Case 1	137.5	37.5	1	0.0	40	90	125.89	62.945	6.31	8.0
Case 2	137.7	38.3		14.5						
Case 3	138.0	39.0		27.5						
Case 4	138.4	39.7		17.0						
Case 5	138.7	40.2		10.0						
Case 6	138.9	40.9		1.0						
Case 7	139.0	41.7		1.0						
Case 8	139.1	42.1		4.0						
Case 9	139.1	42.9		2.0						
Case 10	139.2	43.5		2.0						
Case 11	139.2	44.4		3.0						



(a) Region A



(b) Region F

Figure 2. Computational domain and bathymetry of the East Sea

In order to conduct an accurate safety analysis for Ulchin Nuclear Power Plant site, numerical simulations were carried out for 200 minutes (3 hours 20 minutes). Among three historical and eleven virtual tsunamis, the Central East Sea Tsunami occurred in 1983 and virtual tsunami Case 5 showed higher maximum tsunami heights. Figure 3 represents the maximum tsunami heights obtained by numerical simulation at each point for 2 cases. In order to observe tsunami heights well inside the breakwater, region F was expanded in Figure 3. As shown in Figure 3, the location of the maximum tsunami heights is generated at the most inner of breakwater, and the maximum tsunami heights of 1983 tsunami and Case 5 are approximately 4.4m and 6.3m, respectively. Also, Figure 4 shows the time series of water levels at point A for 2 cases. The initial tsunami arrives about 110 ~ 120 minutes after tsunami occurrence. In Case 5, the maximum amplitude up to 2.7m could be found 40 minutes after the arrival of the first wave.

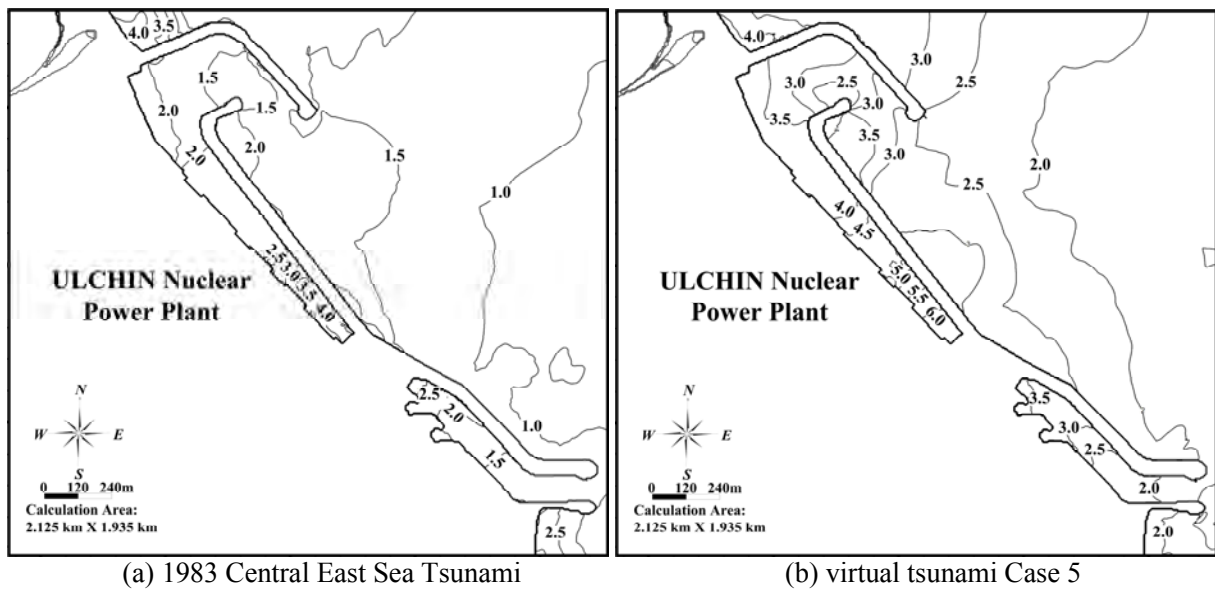


Figure 3. The maximum tsunami heights at each grid point

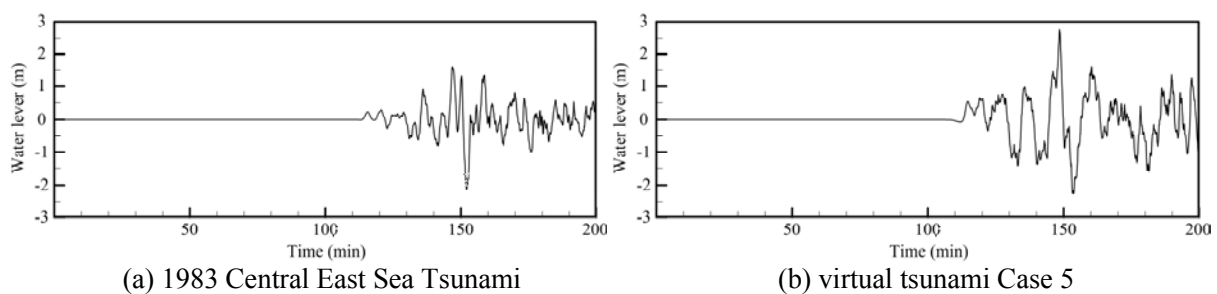


Figure 4. Time series of water levels at point A

CONCLUSION

In this study, a composite numerical model based on the linear shallow-water equations was employed to analyze the safety of the Ulchin Nuclear Power Plant site against three historical and eleven virtual tsunami attacks. The numerical model was computationally efficient through use of the linear

shallow-water equations and dynamic linking method, which allows selecting different mesh sizes within the computational domain.

The results of numerical simulations for three historical and eleven virtual tsunamis are shown that the Ulchin Nuclear Power Plant site is safe at least against those tsunami events. By taking into consideration of the elevation of the Ulchin Nuclear Power Plant site, it can be drawn that the site is safe from those tsunami attacks.

ACKNOWLEDGMENTS

This research was supported by the Research Program through the National Research Foundation of Korea funded by the Ministry of Education, Science and Technology (No. 2011-0015386).

REFERENCE

- Cho, Y.-S. (1995). "Numerical Simulations of Tsunami Propagation and Run-up," Ph.D. theses, Cornell University, USA.
- Cho, Y.-S., Shon, D.-H., and Lee, S. O. (2007). "Practical modified Scheme of linear shallow-water equations for distant propagation of tsunamis," *Ocean Engineering*, Vol. 34, No. 11, pp. 1,769-1,777.
- Imamura, F., Shuto, N. and Goto, C. (1988). "Numerical Simulations of the Transoceanic Propagation of Tsunamis," *In: Proceedings of the 6th Congress Asian and Pacific Regional Division*, IAHR, Japan, pp. 265-272.
- Kajiura, K. and Shuto, N. (1990). "Tsunami," in *The SEA*, edited by B. Le Mehaute, and D. M. Hanes, Vol. 9, Part B, John Wiley & Sons, Inc., pp. 395-420.
- Korean Peninsula Energy Development Organization. (1999). Estimation of Tsunami Height for KEDO LWR Project. Korea Power Engineering Company, Inc., Korea.
- Mansinha, L. and Smylie, D.E. (1971). "The displacement fields of inclined faults," *Bulletin of the Seismological Society of America*, Vol. 61, No. 5, pp. 1,433-1,440.